Quantum confinement and thermal effects on the Raman spectra of Si nanocrystals

Giuseppe Faraci,* Santo Gibilisco, and Agata R. Pennisi
Dipartimento di Fisica e Astronomia, Universitá di Catania, Via Santa Sofia 64, 95123 Catania, Italy and MATIS–Istituto Nazionale di Fisica della Materia, Via Santa Sofia 64, 95123 Catania, Italy

(Received 3 July 2009; revised manuscript received 9 October 2009; published 19 November 2009)

In nanocrystals, first-order Raman spectra can exhibit large shift and width due to two overlapping effects: quantum confinement and thermal heating. In order to distinguish each contribution we studied silicon nanocrystals by Raman spectroscopy. From the measurements we extracted the dependence of the Raman shift and width as a function of the temperature. A model size and temperature dependence was developed for the interpretation of these data, demonstrating the negligible contribution of the quantum confinement for sizes higher then 6 nm. Excellent agreement between theory and experiment was obtained both for the energy shift and for the width broadening.

DOI: 10.1103/PhysRevB.80.193410 PACS number(s): 78.67.Hc, 78.55.Ap, 78.60.−b

Semiconductor nanocrystals are presently of fundamental importance for their innovative properties in applied technology. In particular, clusters, quantum dots, and, in general, crystalline nanoagglomerates of silicon exhibit photoluminescence used in nano-optoelectronic devices. Of course, Si nanocrystals (NCs) are also widely studied from a fundamental point of view for the related quantum size effects.

In this context, the micro Raman technique is a valuable tool for investigating the NCs specific configuration as the Raman peak undergoes an energy shift related to the reduced dimensionality.[1–20] Indeed, in the literature a defined energy shift size dependent was reported. This shift is usually attributed *only* to quantum confinement of the investigated ensemble of NCs. As a matter of fact, another important effect, which can produce a Raman shift, is the possible modification of the local temperature under the laser beam. However, no temperature modification with respect to the ambient temperature has been usually taken into account, because a very low laser radiation fluence is assumed during the Raman measurements. We observe that, even at low laser power, a local increase of the temperature on the illuminated spot can be produced.[21]

In fact, nanocrystals are often surrounded by a layer of oxide acting as a thermal insulator. This can determine radiation trapping and consequent increase in the local temperature. For this reason, it is very important to check the local nanocrystal temperature, as provided by the detection of both Raman (Stokes and anti-Stokes) peaks. As well known, the ratio of these two intensities is directly related to the required local temperature. In these conditions, the two overlapping shifts could be easily disentangled. In our experiment we prepared Si nanocrystals with the aim of clarifying the previous questions. Raman spectra actually confirm a remarkable main peak shift due to a huge temperature increase, even at low laser power. In contrast, the peak shift due to quantum confinement is quite limited and observable only at the lowest sizes.

We prepared silicon NCs using the apparatus described in detail in Ref. 11. A beam of helium, inseminated with silicon vapors, produced clean silicon nanocrystals, expanding in supersonic configuration in a vacuum chamber at a pressure of 10^{-9} Torr. Being synthesized in high vacuum, the clean Si agglomerates were deposited *in situ*, with size in the range 2–12 nm, on a highly oriented pyrolitic graphite (HOPG), quartz, and crystalline Si with native oxide substrates. Several NCs layers were accumulated on these substrates having ascertained that the nanocrystals maintain their individual configuration. Passivation of the surface dangling bonds was obtained through the presence of a low oxygen exposure during cluster evaporation. It is worth noting that this deposition method allows a porous accumulation of many Si nanocrystals of different sizes. Owing to the large size of the experimental spot, the Raman spectra average over the entire size distribution of our clusters. Considering the size distribution of the NCs and the relative volume of each agglomerate, it is obvious that the average is a volume-weighted distribution and therefore the highest sizes preferentially dominate. Therefore, the experimental size distribution has a peak around 10 nm with a dispersion of 4 nm.

For the above samples Raman spectroscopy was applied for detecting the transversal optical (TO) vibrational peak situated for bulk Si at 521 cm^{-1}, when detected at 300 K.

Raman spectra were taken in backscattering geometry with a HORIBA Jobin-Yvon system, equipped with Olympus BX41 microscope. He-Ne laser radiation at a wavelength of 632.8 nm is focused to a spot size of about 3 μm by a 100 $\times$ objective. The laser power on the sample was about 6 mW, and a 550 mm focal length spectrometer with 1800 lines/mm grating was used.

Both absorbed and emitted phonon (anti-Stokes and Stokes) peaks were revealed on several spots of the samples. Moreover, on a fixed spot, a laser beam modification of the power was sufficient to modify the Raman peak position, because of the correlated change of the local temperature.

In Fig. 1 typical Raman spectra are reported for a few temperatures. No difference in the line shape was detected for different substrates. Clearly visible in the figure is how the intensity ratio of the two Raman peaks changes with temperature.

In Fig. 2 the peak position of the Raman spectrum obtained for different silicon nanocrystals deposited on our substrates is reported, as a function of the local temperature deduced by the Stokes/anti-Stokes ratio. As outlined above, by varying the laser power illuminating the single spot, it was possible to modify the temperature, and the related shift, in a range going from the room temperature up to about 800

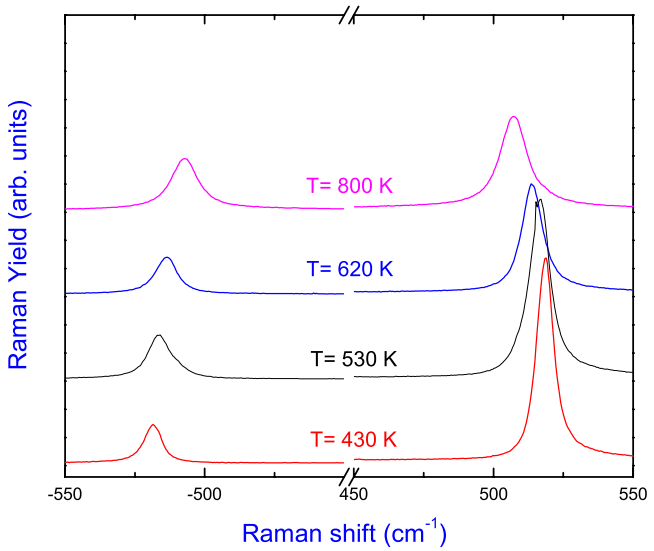

FIG. 1. (Color online) Typical Raman peaks for the temperatures indicated. The local temperature is calculated from the ratio of the Stokes and anti-Stokes peak areas.

K. Note that reference Raman spectra taken on bulk silicon show a peak at ± 521 cm^{-1}, with no shift at any laser power. This is a clear evidence that the bulk crystal is well thermalized, because of its long-range order. In contrast, nanocrystals have short-range order causing a radiation trapping with a consequent local temperature increase.

In Fig. 3 we report the peak width broadening as a function of temperature. Here too we note a large broadening of the Raman peak as the temperature increases, with a higher spread mainly at high temperature. Very likely this can be ascribed to the dispersion of different NCs ensembles.

In order to explain our data, separating, if possible, the different contributions to the energy shift and width broadening, we applied the Raman theory developed in Ref. 20. Here, quantum confinement due to the limited size of the nanocrystals is taken into account. We added to this treatment a dependence on the temperature, following the calculations of Balkanski *et al.*[23]

According to Ref. 20 the Raman spectrum at room temperature is calculated as

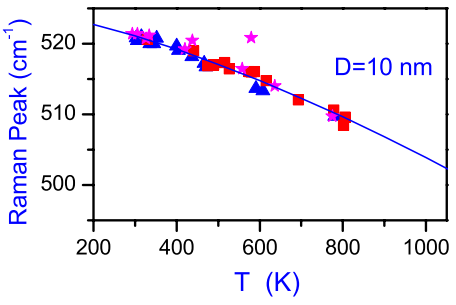

FIG. 2. (Color online) Raman peak position of TO phonons in Si NCs as a function of temperature. The different symbols refer to experimental data from different samples (triangle is used for HOPG substrate, square for quartz, star for silicon substrate). The uncertainty is lower than $\pm 0.1\%$. Also reported by continuous line the theoretical curve calculated for the specified size D=10 nm.

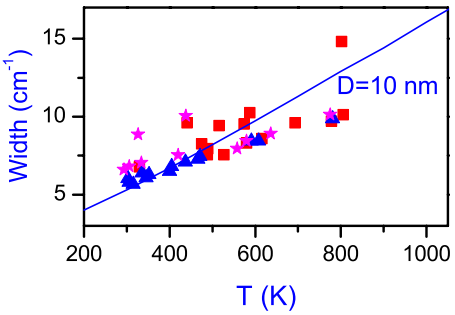

FIG. 3. (Color online) Raman width of the Stokes peak in Si NCs as a function of temperature. The different symbols refer to experimental data for different samples (triangle is used for HOPG substrate, square for quartz, star for silicon substrate). The uncertainty is of the order of $\pm 2.\%$. Also reported by continuous line the theoretical curve calculated for the specified size D=10 nm.

$$I(\omega) \propto \sum_n \int_{(n\pi-1)/D}^{(n\pi+1)/D} \frac{C_n^2(\mathbf{q})d\mathbf{q}}{[\omega-\omega'(\mathbf{q})]^2+(\Gamma/2)^2},$$

where Γ is the natural Lorentzian line shape, including the instrumental resolution, and the phonon dispersion curve $[\omega'(\mathbf{q})]^2$ adopts the analytical form of Ref. 22,

$$[\omega'(\mathbf{q})]^2 = A + B\cos(aq/4)$$

with q in the range $0, 2\pi/a$, $a=0.543$ nm the Si lattice parameter, $A=1.714\times 10^5$ cm^{-2}, $B=1.00\times 10^5$ cm^{-2},

$$C_n(\mathbf{q}) = 3\frac{\sin(qD/2)}{\pi^3 D^3 q(k_n^2-q^2)}.$$

In this approach we assume the phonon wave function in the nanocrystal as a weighted superposition of sinusoidal waves

$$\sum_n \frac{\sin(k_n r)}{k_n r}, \quad \text{for } r \le D/2, \quad \text{or } 0 \text{ otherwise}.$$

with $k_n=n\pi/D$, $n=2,4,6\ldots n\max$ (n max is equal to the maximum integer smaller than $2D/a$ with D diameter of the nanocrystal assumed spherical).

In the previous expressions the temperature dependence of the Raman line position, including anharmonic three-phonon and four-phonon processes, is given by[23]

$$\omega'(\mathbf{q},T) = \omega'(\mathbf{q}) + \Delta(T),$$

where

$$\Delta(T) = \delta_0 + \delta_1\left(1+\frac{2}{e^x-1}\right) + \delta_2\left(1+\frac{3}{e^y-1}+\frac{3}{(e^y-1)^2}\right)$$

and analogously the linewidth

$$\Gamma(T) = \gamma_1\left(1+\frac{2}{e^x-1}\right) + \gamma_2\left(1+\frac{3}{e^y-1}+\frac{3}{(e^y-1)^2}\right),$$

$$x \equiv \hbar\omega'/2k_BT,$$

$$y \equiv \hbar\omega'/3k_BT,$$

where $\delta_{0,1,2}$ and $\gamma_{1,2}$ are constants to be fitted with the experiment.

We obtained the following parameters (in cm^{-1}):

$$\delta_0 = 6.5,$$

$$\delta_1 = 2.96,$$

$$\delta_2 = 0.174,$$

$$\gamma_1 = 2.5,$$

$$\gamma_2 = 0.01.$$

Here, our experimental Raman peak position at 300 K is at $\omega'(\mathbf{q}, 300\ \mathrm{K}) = 521\ \mathrm{cm}^{-1}$, as for bulk silicon. The line width including the experimental resolution broadening is 5.0 cm^{-1}.

The theoretical curves calculated with the above parameters for the average size of our nanocrystals are reported in Figs. 2 and 3 for a comparison with the experimental data. Note that the values of δ_1, δ_2, and γ_1 are the same as in Ref. 23. The value of δ_0 is fixed by the peak position at room temperature. The reduced value of γ_2 can be attributed to a minor contribution of four-phonon processes to the broadening. We note an excellent agreement between theory and experiment for the Raman peak position. Some broadening in the linewidth can be attributed to the size dispersion. For the sake of completeness we report in Fig. 4(a) the theoretical curves calculated for the Raman peak for several sizes as a function of temperature, whereas in Fig. 4(b) the plots are shown as a function of the size for fixed temperature. The calculated curves demonstrate a quantum confinement effect mainly for sizes lower than about 6 nm. Note the reduced shift at fixed temperature between the theoretical data, which undergo quantum size effects progressively smaller as the NCs size reaches about 10 nm. Beyond 10 nm nanocrystal size negligible quantum confinement effects can be detected. In contrast, local heating has an enormous influence even at high size, with a shift larger than 10 cm^{-1} going from ambient temperature up to 800 K. We emphasize that the present results are in contrast with those published in Ref. 21, where only qualitative values along the correct trend can be found.

We briefly discuss our data pointing out the important results obtained by the present experiment, corroborated by the model we developed for its interpretation. We demonstrated the negligible contribution of quantum confinement effects both to the Raman shift and to the line broadening for Si NCs size higher than about 6 nm. Actually, the effects such as line shift and broadening are to be ascribed to the local temperature increase in the nanocrystals ensembles even at low laser irradiation. This point is related to the cluster morphology. Being the nanocrystal deposition quite porous, and each agglomerate surrounded by a thin oxide layer, the local increase in temperature is determined by radiation trapping. This does not happen in bulk silicon because of the efficient energy exchange due to long-range order. The present measurements also demonstrate the possible presence in the literature of large overestimation of quantum confinement effects with respect to simple local heating. These two contributions to the Raman shift are actually overlapped. It is therefore imperative to determine for the NCs ensemble the real temperature through the detection of both Raman peaks. In conclusion, we reported data for the Raman energy shift in Si NCs, to be assigned not to size effects as often claimed in the literature, but to the NCs temperature. In no case the reduced laser power rate can justify the attribution of Raman shifts to quantum confinement effects, size (and not temperature) dependence.

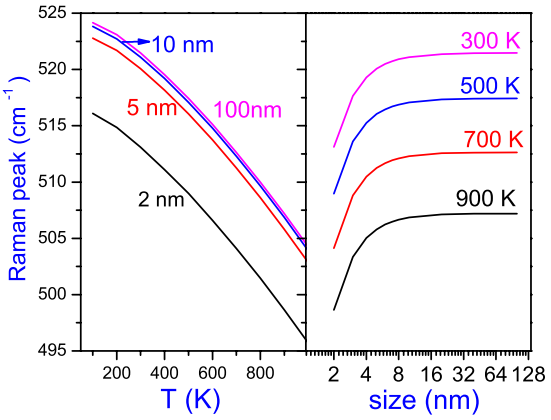

FIG. 4. (Color online) Raman peak position calculated by the present theory (a) for the specified size as a function of temperature, (b) for the specified temperature as a function of the size.

*giuseppe.faraci@ct.infn.it

[1] M. Ehbrecht, H. Ferkel, F. Huisken, L. Holz, Yu. N. Polivanov, V. V. Smirnov, O. M. Steimakh, and R. Schmidt, J. Appl. Phys. **78**, 5302 (1995).

[2] M. Ehbrecht, B. Kohn, F. Huisken, M. A. Laguna, and V. Paillard, Phys. Rev. B **56**, 6958 (1997).

[3] V. Paillard, P. Puech, M. A. Laguna, R. Carles, B. Kohn, and F. Huisken, J. Appl. Phys. **86**, 1921 (1999).

[4] Hua Xia, Y. L. He, L. C. Wang, W. Zhang, X. N. Liu, X. K. Zhang, D. Fang, and Howard E. Jackson, J. Appl. Phys. **78**, 6705 (1995).

[5] W. Cheng and S.-F. Ren, Phys. Rev. B **65**, 205305 (2002).

[6] J. Zi, K. Zhang, and X. Xie, Phys. Rev. B **55**, 9263 (1997).

[7] Jian Zi, H. Büscher, C. Falter, W. Ludwig, Kaiming Zhang, and Xide Xie, Appl. Phys. Lett. **69**, 200 (1996).

[8] Takafumi Seto, Takaaki Orii, Maroto Hirasawa, and Nobuhiro Aya, Thin Solid Films **437**, 230 (2003).

[9] M. Perego, S. Ferrari, M. Fanciulli, G. Ben Assayag, C. Bonafos, M. Carrada, and A. Claverie, J. Appl. Phys. **95**, 257 (2004).

[10] H. Richter, Z. P. Wang, and L. Ley, Solid State Commun. **39**, 625 (1981).

[11] A. R. Pennisi, P. Russo, S. Gibilisco, G. Compagnini, S. Battiato, R. Puglisi, S. La Rosa, and G. Faraci, in *Conference Proceedings on Progress in Condensed Matter Physics*, edited by G.

Mondio and L. Silipigni (SIF Bologna, Italy, 2003), Vol. 84, p. 183; G. Faraci, S. Gibilisco, P. Russo, A. R. Pennisi, G. Compagnini, S. Battiato, R. Puglisi, and S. La Rosa, Eur. Phys. J. B **46**, 457 (2005).

[12] Y. Guyot, B. Champagnon, M. Boudeulle, P. Mélinon, B. Prével, V. Dupuis, and A. Perez, Thin Solid Films **297**, 188 (1997).

[13] Z. Iqbal, S. Veprek, A. P. Webb, and P. Capezzuto, Solid State Commun. **37**, 993 (1981).

[14] M. Fujii, Y. Kanzawa, S. Hayashi, and K. Yamamoto, Phys. Rev. B **54**, R8373 (1996).

[15] G. H. Li, K. Ding, Y. Chen, H. X. Han, and Z. P. Wang, J. Appl. Phys. **88**, 1439 (2000).

[16] P. Parayanthal and Fred H. Pollak, Phys. Rev. Lett. **52**, 1822 (1984).

[17] J. H. Campbell and P. M. Fauchet, Solid State Commun. **58**, 739 (1986).

[18] A. A. Sirenko, J. R. Fox, I. A. Akimov, X. X. Xi, S. Rumirov, and Z. Liliental-Weber, Solid State Commun. **113**, 553 (2000).

[19] Peter Y. Yu and Manuel Cardona, *Fundamentals of Semiconductors* (Springer, Berlin, 1996).

[20] G. Faraci, S. Gibilisco, P. Russo, A. R. Pennisi, and S. La Rosa, Phys. Rev. B **73**, 033307 (2006).

[21] M. J. Konstantinovic, S. Bersier, X. Wang, M. Hayne, P. Lievens, R. E. Silverans, and V. V. Moshchalkov, Phys. Rev. B **66**, 161311(R) (2002).

[22] R. Tubino, P. Piseri, and G. Zerbi, J. Chem. Phys. **56**, 1022 (1972).

[23] M. Balkanski, R. F. Wallis, and E. Haro, Phys. Rev. B **28**, 1928 (1983).